J. Plasma Phys. (2018), *vol.* 84, 905840610
doi:10.1017/S0022377818001162

On annihilation of the relativistic electron vortex pair in collisionless plasmas

K. V. Lezhnin[1,2,†], F. F. Kamenets[3], T. Zh. Esirkepov[4] and S. V. Bulanov[4,5,6]

[1]Department of Astrophysical Sciences, Princeton University, Princeton, NJ 08544, USA

[2]National Research Nuclear University MEPhI, Kashirskoe sh. 31, 115409, Moscow, Russia

[3]Moscow Institute of Physics and Technology, Institutskiy per. 9, Dolgoprudny, Moscow Region 141700, Russia

[4]National Institutes for Quantum and Radiological Sciences and Technology, 8-1-7 Umemidai, Kizugawa, Kyoto 619-0215, Japan

[5]Institute of Physics of the Czech Academy of Sciences v.v.i. (FZU), Na Slovance 1999/2, 18221, Prague, Czech Republic

[6]Prokhorov General Physics Institute of the Russian Academy of Sciences, 119991 Moscow, Russia

(Received 7 September 2018; revised 25 October 2018; accepted 29 October 2018)

In contrast to hydrodynamic vortices, vortices in a plasma contain an electric current circulating around the centre of the vortex, which generates a magnetic field localized inside. Using computer simulations, we demonstrate that the magnetic field associated with the vortex gives rise to a mechanism of dissipation of the vortex pair in a collisionless plasma, leading to fast annihilation of the magnetic field with its energy transforming into the energy of fast electrons, secondary vortices and plasma waves. Two major contributors to the energy damping of a double vortex system, namely, magnetic field annihilation and secondary vortex formation, are regulated by the size of the vortex with respect to the electron skin depth, which scales with the electron γ factor, γ_e, as $R/d_e \propto \gamma_e^{1/2}$. Magnetic field annihilation appears to be dominant in mildly relativistic vortices, while for the ultrarelativistic case, secondary vortex formation is the main channel for damping of the initial double vortex system.

Key words: plasma nonlinear phenomena, plasma simulation, plasma waves

1. Introduction

Formation and evolution of localized nonlinear structures such as vortices and solitons play a crucial role in the physics of continuous media (Saffman 1993; Nettel 2009). For instance, drift wave dynamics in tokamak plasmas can be described within the framework of the Hasegawa–Mima (HM) equation (Hasegawa & Mima 1978), which has a well-known point-vortex solution. The vortices may affect energy and particle transport significantly (Nycander & Isichenko 1990; Hobson 1991; Kono & Horton 1991; Krasheninnikov 2016; Zhang & Krasheninnikov 2016). The formation of finite-radius relativistic electron vortex structures associated with quasistatic magnetic

† Email address for correspondence: klezhnin@princeton.edu

field generation provides one of the pathways for the electromagnetic field energy depletion in laser plasmas (Bulanov *et al.* 1996). The late stage of the vortex evolution resulting in strong plasma density modulations has been revealed in experiments (Romagnani *et al.* 2010; Sylla *et al.* 2012) using proton radiography. Electron vortex pairs are also observed in simulations of relativistic shocks, being responsible for electron energization in the upstream region (Naseri *et al.* 2018). Understanding the dynamics of vortex structures in plasmas is important for developing the theory of relativistic plasma turbulence (Bulanov *et al.* 1997; Kuvshinov & Schep 2016). Relativistic electron vortex dynamics may also be a significant factor in the late stages of the relativistic Weibel-like instability (Califano, Pegoraro & Bulanov 1997), which can arise in superstrong laser–plasma interactions (Wei *et al.* 2004), as well as in colliding astrophysical flows of electron–positron plasmas (Kazimura *et al.* 1998).

In contrast to hydrodynamical vortices, which are sustained by fluids comprised of neutral particles, vortices in plasmas are sustained by the rotational motion of charged particles, leading to a non-zero circular electric current, which forms a magnetic field inside the vortex (Lezhnin *et al.* 2016). In the case of small radius vortices, which correspond to the point-vortex solution of the HM equation, the vortex internal energy is conserved during the interaction process. However, in the case of finite-radius vortices, we expect the finite-radius and electromagnetic interaction effects to become prominent, leading to a fast vortex energy dissipation with its transformation into the energy of fast particles. Below, using two-dimensional (2-D) particle-in-cell (PIC) simulations with the code REMP (Esirkepov 2001), we demonstrate how pairs of vortices interact beyond the point-vortex approximation. We reveal the effect of relativistic annihilation of the binary electron vortices' magnetic field that leads to vortex pair dampening.

2. Simulation set-up

In order to consider an interaction of initially isolated stationary electron vortices, we take advantage of the well-known property of the finite-radius vortex motion in a medium with a density gradient – vortices in such a medium tend to drift with constant velocity perpendicular to the density gradient due to conservation of Ertel's invariant (Ertel 1942), or due to conservation of a generalized magnetohydrodynamic version of Ertel's invariant, Hide's invariant (Hide 1983; Pegoraro 2018). After initializing two stationary electron vortices far away from each other, their drift motion will slowly bring them close enough for interaction to happen.

The simulation parameters are as follows. For the clarity and reproducibility of our numerical simulations, we describe the simulation set-up in terms of an arbitrary spatial scale parameter, λ, and then immediately rescale the model to the physically relevant units. We set a slab of electron plasma (assuming immobile ions) with a constant density gradient along the x axis, so the electron plasma density equals $n_e/n_{\max} = 0.1$ at $x = 55\lambda$ and $n_e/n_{\max} = 1$ at $x = 95\lambda$, with width 40λ and zero temperature for the electrons. We measure spatial parameters in λ, temporal – in $2\pi/\omega_0 = \lambda/c$, densities – in $n_0 = m_e\omega_0^2/4\pi e^2$, electromagnetic fields – in $E_0 = m_e\omega_0 c/e$, where m_e is electron mass, e is the absolute value of electron charge, c is the speed of light in a vacuum. For the sake of simplicity, we introduce circularly symmetric electron vortices. They are initiated by accumulating the localized magnetic field during a number of time steps at the beginning of the simulation (Bulanov *et al.* 2006; Lezhnin *et al.* 2016). For the simulations presented, electron vortices are formed with various maximum magnetic fields: $B_{\max} = 0.5, 1, 2, 4, 6.5, 35$ in plasmas

https://doi.org/10.1017/S0022377818001162 Published online by Cambridge University Press

with $n_{\max} = 0.16, 0.36, 0.64, 1, 4, 16$, respectively. Hereafter, we will refer to the simulation parameters by the magnetic field amplitude $B_{\max}$. The vortex centres are located around points $x = 75\lambda$ and $y = -4\lambda, 4\lambda$. We choose our parameters in such a way that the condition $\omega_{\rm pe}^2 \ll \omega_B^2$ holds (Gordeev 2010), so the electrons can be considered magnetized. Here $\omega_{\rm pe}^2 = 4\pi n_e e^2/m_e$ is the plasma frequency and $\omega_B = eB/m_e c$ is the electron gyrofrequency. The computational grid is $150\lambda \times 120\lambda$ with 32 nodes per λ, and the boundary conditions are periodic. We have also qualitatively verified the results of our simulations with a larger domain resolution (64 and 128 nodes per λ). The initial particle-in-cell number corresponding to the maximum electron density is equal to 100. The total number of particles is approximately 10^8. The integration time step is 0.0155. The total time of the simulations is 500 time units. We have also verified our results for similar simulation parameters with the code EPOCH (Ridgers *et al.* 2014).

For the sake of clarity, we further rescale our numerical model to physically relevant units appearing from the simple electron vortex model. It can be formulated as follows. Let us assume that the electron moves in a circular orbit around the uniformly distributed immobile and positively charged ions. Then, the electric field experienced by the electron is $E = 2\pi enR$, where R is the radius of the electron vortex and n is the ion density. Assuming the electron to have a speed $v_e \approx v_{E\times B} = cE \times B/B^2 \sim c$, yields $B \sim E = 2\pi enR$. Radial force balance for the electron can be written as $v_e p_e/R = -eE$, which gives an expression connecting the electron vortex radius and electron momentum, $R = (p_e c/2\pi ne^2)^{1/2} \approx d_e\sqrt{2\gamma_e}$. Thus, we fix $\lambda = (4\pi^2 n_{\max}/n_0 \cdot m_e c/p_e)^{1/2} R$, normalizing all spatial quantities by R, temporal frequencies by crossing frequency $\omega_{cr} = c/R$, fields by $E_0' = m_e\omega_{cr}c/e$, densities by $n_0' = m_e\omega_{cr}^2/4\pi e^2$. It is also worth noting that the vortex size in terms of local electron skin depth, R/d_e, in our simulations is proportional to $B_{\max}/n_{\max}^{1/2}$, so larger $B_{\max}$ correspond to larger vortices with respect to d_e.

3. PIC simulation results and theoretical estimates

In our simulations, we expect to observe the following scenario: first, when two vortices are far away from each other ($>5R$), they would be stationary unless we were to take into account the effects of a finite vortex radius. In the latter case, we can expect that the vortices will move perpendicularly to the density gradient (parallel to the y-axis), due to the conservation of Ertel's invariant $I = \Omega/n$, where Ω is the vorticity and n is the plasma density (Ertel 1942). The velocity of such motion is estimated as $\Omega R^2|\nabla n/n|$, which is $\lessapprox c/80$ and has turned out to be fairly consistent with the simulation results presented below. On the other hand, Hide's invariant, $I_{\rm H} = B/n$, will lead to the following drift velocity: $\omega_B R^2|\nabla n/n|$. Comparison of the electron gyrofrequency with the electron vorticity in the case of a relativistic plasma will give $|\omega_B|/|\Omega| = \omega_B/|\nabla \times p_e/m_e| \approx \omega_B/|\nabla \times c\beta_e\gamma_e| \approx \omega_B R/c\gamma_e \approx \omega_B/\gamma_e\omega_{\rm cr} \sim 1$ in the case of our simulations. The same can be shown from our analytical estimates by inserting expressions for B and R into the $|\omega_B|/|\Omega|$ ratio. Thus, the Ertel and Hide invariants lead to approximately equal electron vortex drift velocities, but, in principle, a more sophisticated theory is required to accurately describe a finite-radius electron vortex drift motion with finite charge separation in the vortex core and relativistic electron energies.

Then, when the vortex interaction becomes significant (it scales as $\mathrm{K}_0(|\Delta y/d_e|)$ with the vortex separation Δy, where K_0 is the modified Bessel function of the second kind, see e.g. Kono & Horton (1991)), we expect the binary vortex to start moving along

https://doi.org/10.1017/S0022377818001162 Published online by Cambridge University Press

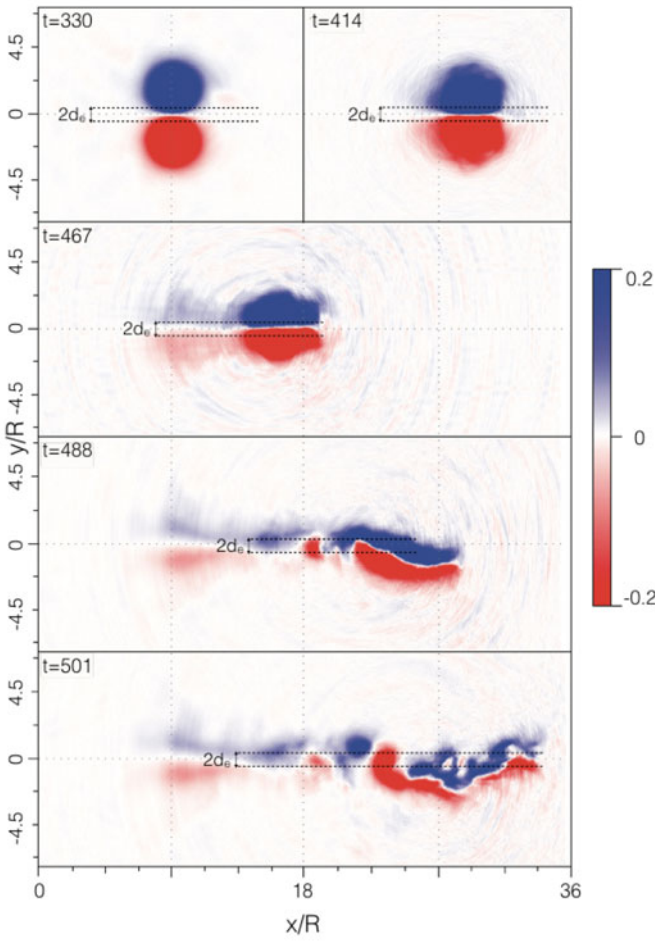

FIGURE 1. Sketch of the binary vortex evolution – z component of the magnetic field: approaching each other ($t = 330$), formation of the dipole vortex structure ($t = 414$), radiation of electromagnetic waves and formation of a dipole magnetic field structure in the wake of the dipole vortex ($t = 467$), decay of the dipole vortex into smaller electron vortices, which form von Kármán vortex rows ($t = 488$), and the magnetic field annihilation, leading to electron heating ($t = 501$). The $2d_e$ width scale, tightly connected to the annihilation process, is demonstrated.

the x axis and possibly follow one of the complicated trajectories discussed in Kono & Horton (1991). The typical velocities of such motion are $V_{\text{bin}} \approx 0.2$–$0.5c$. Eventually, the vortex binary tightening until $\sim R$ will lead to the finite-radius effects coming into play, which are beyond the scope of applicability of the point-vortex theory described in Kono & Horton (1991). To reveal the finite vortex radius effects and the effects of magnetic interaction we perform the PIC simulations.

Figure 1 illustrates the typical evolution of the B_z component of the magnetic field observed during the simulation (for $B_{\max} = 2$). When the binary vortex system is tight enough (i.e. distance between the closest points of the vortices is $\sim d_e$, where $d_e = c/\omega_{\text{pe}}$ is the electron skin depth, figure 1, $t = 330$), the point-vortex approximation breaks down. The electron currents of the two vortices, both directed along the x axis

https://doi.org/10.1017/S0022377818001162 Published online by Cambridge University Press

at the closest point of approach, attract each other and form a magnetic-dipole vortex structure (figure 1, $t = 414$) (Naumova *et al.* 2001; Nakamura & Mima 2008). The structure observed has an analogue in hydrodynamics, which is known as the Larichev–Reznik dipole vortex solution (Larichev & Reznik 1976). This type of structure is believed to be stable in the hydrodynamic case (McWilliams *et al.* 1981). However, in our case, the magnetic structure moves along the $+x$ direction, losing the majority of its magnetic energy by turning it into electromagnetic waves (figure 1, $t = 467$; figure 3*b*), accelerated electrons and the formation of von Kármán-like streets of secondary vortices (figure 1, $t = 488$, 501; figure 3*b*,*c*), although secondary vortex formation does not decrease the total magnetic energy of the system significantly. The direction of the binary vortex motion may be deflected from straight propagation along the x axis, as the binary components disintegrate unequally on the secondary vortices, and the resulting binary vortex with unequal components deflects in the direction of the larger vortex component, in agreement with Kono & Horton (1991). The rapidly accelerated electrons are a sign of the relativistic magnetic field annihilation. The annihilation of the magnetic field was observed in PIC simulations previously in a different geometry (Gu *et al.* 2016) between the azimuthal magnetic fields formed by two parallel laser pulses propagating in a non-uniform underdense plasma and leads to electron heating. Although the overall physics of Ampere's law is the same in both cases, as well as the signature of rapid electron energization, in Gu *et al.* (2016) the displacement current arose as a result of the magnetic fields expanding towards each other due to the negative density gradient along the propagation axis of the laser pulses. In our case, the two vortices are pushed towards each other by the finite-radius effect of the vortex drift motion and continue to squeeze after the dipole vortex formation (see figure 1), so the gradient in the magnetic field cannot be compensated solely by increase of the electron current between the dipole vortex components. Still, in both cases, the dynamics of the magnetic fields is guided by the conservation of Ertel's invariant. The process of secondary vortex formation may be caused by vortex boundary bending, observed in simulations previously (Lezhnin *et al.* 2016). Secondary vortices are not subject to the vortex film instability (Bulanov *et al.* 1996), as the finite vortex radius effects dominate the motion of the vortices which are separated by a few d_e. The role of the relativistic effects is demonstrated using auxiliary simulations with $n_{\max} = 0.36$ with a large range of $B_{\max}$ from 0.1 to 2, with R/d_e here being $\leqslant 1$. It was demonstrated that the magnetic field damping in the non-relativistic case is at least three times longer, and the electric fields coming from the displacement current term in Ampere's law are negligible, see Wang *et al.* (2016).

A simple model of the magnetic field annihilation of electron vortices may be written as follows. The radius of a vortex is connected to the electron momentum by the relation $R/d_e = (2p_e/m_e c)^{1/2}$. Thus, the non-relativistic vortices have radius $R \leqslant d_e$ and the ultrarelativistic vortices have $R \gg d_e$. Ampere's law is generally stated as $\nabla \times \boldsymbol{B} = 4\pi/c \cdot \boldsymbol{J} + 1/c \cdot \partial \boldsymbol{E}/\partial t$. It may be rewritten as an order-of-magnitude estimate, using $|\nabla \times \boldsymbol{B}| \approx |\partial B/\partial y| \sim |B/d|$, where d is the typical spatial gradient scale length, $|\boldsymbol{J}| \approx e n_e c$ for the limit when $v_e \sim c$, $|\partial \boldsymbol{E}/\partial t| \sim E/\tau$, where τ is the typical temporal scale. Finally, this yields $d/d_e = \hat{B}/(1 + \hat{E}/\omega_{\mathrm{pe}}\tau)$ ($\hat{B}$ and $\hat{E}$ are dimensionless). Thus, it is clear from this equation that reaching d_e scale ($d \leqslant d_e$) is necessary for the magnetic field annihilation through the displacement current term (see, e.g. Gu *et al.* 2016; Wang *et al.* 2016). In the case of our simulations, the ratio of the $\nabla \times B$ term to the current term with the increased density can be written as (by an order of magnitude): $|\nabla \times \boldsymbol{B}|/|4\pi/c \cdot \boldsymbol{J}| \sim |B/d|/|4\pi\alpha n_e e| \sim \hat{B} \cdot (d_e/d) \cdot (1/\alpha)$, where α accounts for possible increase of the current due to the increase in electron density

https://doi.org/10.1017/S0022377818001162 Published online by Cambridge University Press

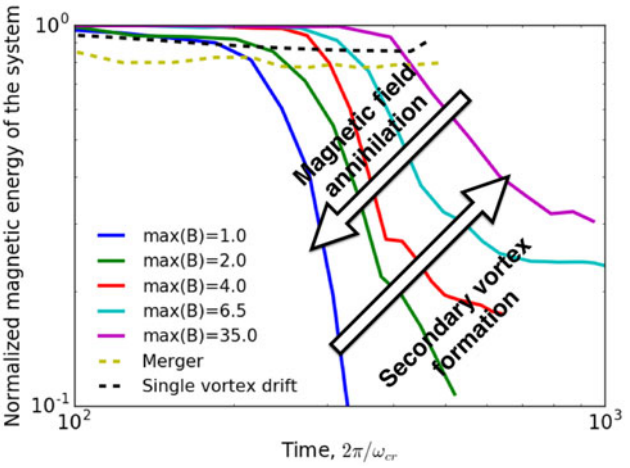

FIGURE 2. Normalized magnetic field energy evolution over time for various cases – drifting single vortices (dashed black line), merging vortices (dashed brown line), dissipating vortices for $B_{\max} = 1.0$ (blue), $B_{\max} = 2.0$ (green), $B_{\max} = 4.0$ (red), $B_{\max} = 6.5$ (aqua) and $B_{\max} = 35$ (purple). In the case of smaller vortices (in terms of $R/d_e \propto B_{\max}$) the magnetic field annihilation dominates the vortex damping, in the case of larger density values – secondary vortex formation mitigates the total magnetic energy dissipation.

with $\alpha \leqslant 2$ in our simulations. This parameter is > 5 in our small $B_{\max}$ simulations (as, for instance, shown at figure 1 for $B_{\max} = 2$ case) and ~ 1 in large $B_{\max}$ simulations (as in the $B_{\max} = 35$ case). Thus, the more relativistic the vortex is (in terms of the $p_e/m_e c \approx \gamma$ parameter), the harder it is to squeeze the dipole vortex down to a d_e scale. That being said, large vortices (in terms of d_e scale) are harder to damp via the magnetic field annihilation.

Let us compare two types of simulations with the same parameters except for the signs of the magnetic fields in the vortices. Thus, in one case the vortices move towards each other and interact (figure 2, blue line), in the other case they move away from each other and do not decay on the time scale of the simulations (figure 2, dashed black line). Figure 2 shows the rate of magnetic energy dissipation in both simulations. Here, we can distinguish at least two mechanisms of vortex dissipation – slow (dashed lines, dissipation time is larger than $10^3\omega_{cr}^{-1}$) and fast (solid lines, typically less or much less than $10^3\omega_{cr}^{-1}$). The first mechanism can probably be attributed to the formation of electrostatic spiral density waves in the electron plasma, which are seen in the early stages of the simulations (e.g. see spiral perturbations of electron density in figures 3*a* and 4*a*). In our simulations, this mechanism gives us the rate of dissipation which dissipates no more than 20 % of the magnetic energy during the simulation time, so it will not impact the characteristic lifetime of the electron vortex, or at least will make a contribution on a longer time scale than the fast dissipation, which will be discussed below. In turn, fast vortex dissipation can destroy the vortex pair on a much shorter time scale. Synchrotron losses, in contrast to electromagnetic solitons, are also negligible in the electron vortex case (Esirkepov *et al.* 2004). Using two-dimensional EPOCH simulations that include synchrotron radiation with single vortex drift in the plasma density gradient, we have shown that for a $B_0 \sim 10$ vortex with a given set of parameters, the synchrotron damping of vortex energy is no more than 0.1 % of total vortex energy for 500 crossing times.

https://doi.org/10.1017/S0022377818001162 Published online by Cambridge University Press

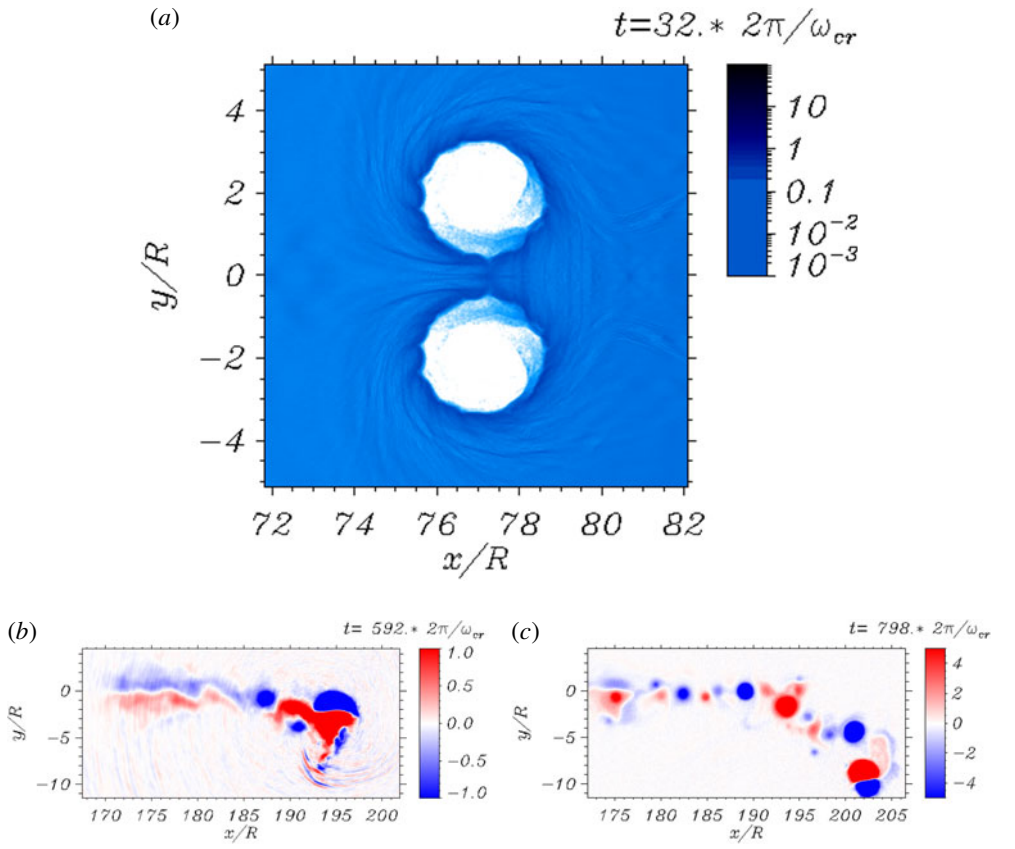

FIGURE 3. (*a*) Electron density distribution for $t = 32$ (simulation with $B_{\max} = 0.5$). Spiral density waves, which possibly correspond to the electromagnetic energy dissipation mechanism at the early stages of vortex evolution, are seen; (*b*) B_z component of the magnetic field for $t = 592$ (simulation with $B_{\max} = 6.5$). Around $x = 193$ and $y = -8$ we observe the emission of the electromagnetic wave. (*c*) B_z component of the magnetic field for $t = 798$ (simulation with $B_{\max} = 35.0$). The von Kármán-like street of secondary vortices is observed in the wake region of the dipole vortex.

As a result of the magnetic energy dissipation, we observe a bunch of electrons being accelerated approximately in the $+x$ direction, adding up to $\sim 60 m_e c$ to the electron momentum in comparison to the maximum electron momentum of the stationary electron vortices in the case of $B_{\max} = 35$. Figure 4 demonstrates the effect of the electron acceleration. The energy of the electrons is large enough for the bunch to escape the plasma region. According to figure 2, we see that the more relativistic vortices, with larger γ factors, are harder to annihilate, in agreement with our theoretical model. Secondary vortices, which are more prominent in the simulations with higher γ factors of the initial vortices, are also more stable against magnetic field annihilation, which results in the saturation of the magnetic field energy in the system (see figure 2, aqua and purple lines).

It is also important to note that the immobile ion approach is justified only if $\omega_{\rm pi}/\omega_{\rm pe} \ll 1$ and $2\pi/\omega_{\rm pi}$ is greater than the total simulation time. Besides, the binary vortex motion should be fast enough so that we could ignore the ion motion: $V_{\rm bin}/R \gg \omega_{\rm pi}$, where R is the typical radius of the vortex. Otherwise, the binary

https://doi.org/10.1017/S0022377818001162 Published online by Cambridge University Press

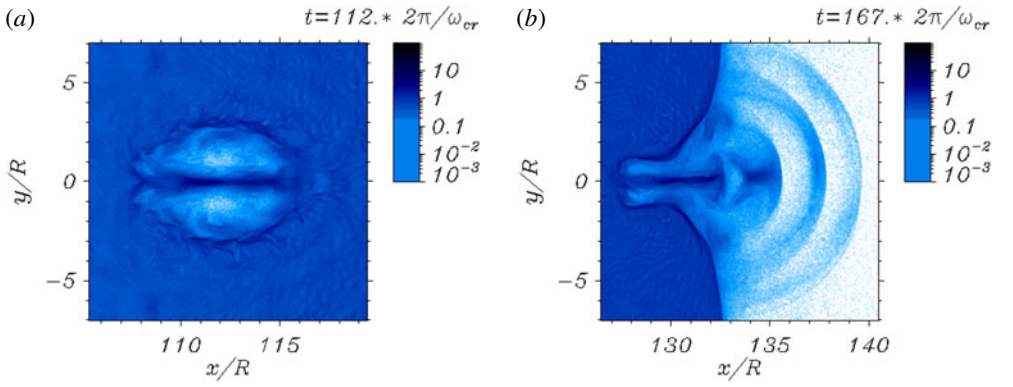

FIGURE 4. Electron density distribution at (*a*) $t = 112$ and (*b*) $t = 167$ ($B_{\max} = 4$ simulation). The annihilation of the magnetic field leads to the formation of an electron bunch with an energy allowing escape of the plasma into the vacuum.

system of vortices does not move according to the HM equation, and the vortices evolve independently (Lezhnin *et al.* 2016) until two vortex boundaries collide. Figure 5 shows the ion acceleration from the interaction of two exploding relativistic electron vortices in our EPOCH simulations with mobile protons. Here, we take $n_e = 4 \cdot n_{\rm cr}$, $B_{\max} \sim 10$, the simulation box is 800×400 grid nodes, corresponding to $40\lambda \times 20\lambda$ physical size ($\lambda = 1$ μm), with 200 particles per cell, and we keep the plasma in the left side of the simulation box, while forming vortices at $x = 10\lambda$ and $y = -3\lambda, +3\lambda$ with opposite signs of the magnetic field. Two vortices with the initial field amplitude of $B_{\max} \sim 10$ approach each other during the explosion, and some sort of dipole structure is separated from the vortex pair, moving to the plasma boundary and damping its magnetic energy into particles. Asymmetry of magnetic field distributions demonstrates the role of the dipole vortex, which leads to higher energies of protons from the right side, as shown in the phase plot, figure 5(*d*), in comparison to the contribution of the Coulomb explosion, which is seen as a circular structure in the phase plot. This mechanism is similar to the so-called magnetic vortex acceleration (MVA) (Fukuda *et al.* 2009; Bulanov *et al.* 2010; Nakamura *et al.* 2010). An alternative mechanism of ion acceleration from relativistic electron vortex pairs was recently considered in Yi *et al.* (2018).

The simulation set-up used in the problem, such as a plasma density gradient, is implemented in order to consider the adiabatic switching on of the vortex interaction effects. Thus, we may observe the same effect of vortex damping in homogeneous plasmas when forming tight binary systems of vortices using our numerical scheme. However, in order to exclude the effect of the initial generation process, which inevitably will cause strong coupling between the vortex pair, and to demonstrate the stability of single electron vortices, we decided to form vortices far away from each other, making sure that the vortex generation process does not impact their interaction and the magnetic field energy is almost constant over the simulation time (for non-interacting vortices). The dashed black line in figure 2 demonstrates the evolution of the magnetic energy in the single vortex drift case. In general, the lifetime of electron vortex binaries in a homogeneous plasma appears to be longer than in the non-zero density gradient case.

It is also natural to discuss a system of binary vortices with the same polarization of magnetic field. In the point-vortex approximation, they will simply rotate around

https://doi.org/10.1017/S0022377818001162 Published online by Cambridge University Press

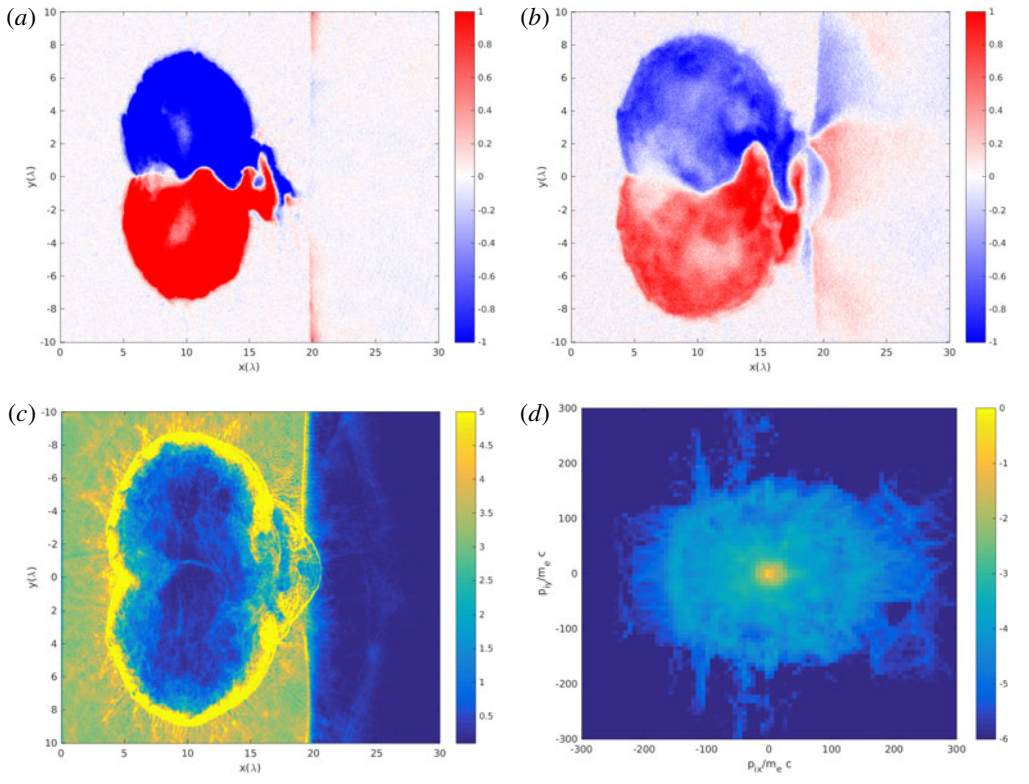

FIGURE 5. Ion acceleration in a vortex pair interaction: magnetic field distribution at (*a*) $t = 300$ fs, (*b*) $t = 600$ fs, (*c*) proton density distribution at $t = 600$ fs and (*d*) p_{ix}–p_{iy} phase plot at $t = 600$ fs.

each other in the case of a homogeneous plasma (Kono & Horton 1991). However, it turns out that the finite-radius vortices are subject to a merger process, which may also lead to minor electromagnetic energy dissipation (figure 2, dashed brown line) via spiral density wave formation by the resulting ellipsoidal vortex (Lezhnin *et al.* 2017), which turned out to be in principle agreement with the results of the hydrodynamical simulations of the 2-D vortex merger process (Overman II & Zabusky 1982).

4. Conclusions

In conclusion, we presented the computer simulation results on the interaction of electron vortex binaries. These structures are often seen in 2-D PIC simulations of various laser–plasma configurations and are crucial for understanding the superstrong magnetic field evolution and turbulence in relativistic plasmas. If the binary vortex system is tight enough, the point-vortex approximation breaks down, and the binary vortex is subject to fast annihilation. The vortex annihilation leads to acceleration of the electron bunches, which in its turn leads to propagating electrostatic waves. In the case of larger γ factor of the initial vortices (i.e. for simulations with $B_{\max} = 4$ and above), we also observe formation of von Kármán streets of secondary vortices, the motion of which is stabilized by the drift motion due to the finite-radius effects. Mildly relativistic electron vortex pairs damp mainly through the annihilation of the

https://doi.org/10.1017/S0022377818001162 Published online by Cambridge University Press

magnetic field, while ultrarelativistic electron vortex pairs decay via the secondary vortex formation. We also show that in the mobile proton simulations that magnetic field annihilation contributes to the ion acceleration in the exploding vortex pair set-up. We believe that the results obtained will be useful for the development of a theory describing electromagnetic turbulence in relativistic plasmas (Bulanov *et al.* 1997; Kuvshinov & Schep 2016; Naseri *et al.* 2018).

Acknowledgements

This work utilized the MIPT-60 cluster, hosted by the Moscow Institute of Physics and Technology (we thank I. Seleznev for running it smoothly for us). S.V.B. acknowledges support at the ELI-BL by the project High Field Initiative (CZ.02.1.01/0.0/0.0/15_003/0000449) from the European Regional Development Fund. K.V.L. is grateful to the ELI-Beamlines project for hospitality during the final stages of this work. K.V.L. thanks V. Blinov for fruitful discussions.

REFERENCES

Bulanov, S. S., Bychenkov, V. Y., Chvykov, V., Kalinchenko, G., Litzenberg, D. W., Matsuoka, T., Thomas, A. G. R., Willingale, L., Yanovsky, V., Krushelnick, K. *et al.* 2010 Generation of gev protons from 1 pw laser interaction with near critical density targets. *Phys. Plasmas* **17** (4), 043105.

Bulanov, S. S., Esirkepov, T. Z., Kamenets, F. F. & Pegoraro, F. 2006 Single-cycle high-intensity electromagnetic pulse generation in the interaction of a plasma wakefield with regular nonlinear structures. *Phys. Rev.* E **73**, 036408.

Bulanov, S. V., Esirkepov, T. Zh., Lontano, M. & Pegoraro, F. 1997 The stability of single and double vortex films in the framework of the Hasegawa–Mima equation. *Plasma Phys. Rep.* **23**, 660.

Bulanov, S. V., Lontano, M., Esirkepov, T. Zh., Pegoraro, F. & Pukhov, A. M. 1996 Electron vortices produced by ultra intense laser pulses. *Phys. Rev. Lett.* **76**, 3562.

Califano, F., Pegoraro, F. & Bulanov, S. V. 1997 Spatial structure and time evolution of the weibel instability in collisionless inhomogeneous plasmas. *Phys. Rev.* E **56**, 963–969.

Ertel, H. 1942 Ein neuer hydrodynamischer Wirbelsatz. *Meteorol. Z.* **59**, 277.

Esirkepov, T., Bulanov, S. V., Nishihara, K. & Tajima, T. 2004 Soliton synchrotron afterglow in a laser plasma. *Phys. Rev. Lett.* **92**, 255001.

Esirkepov, T. Zh. 2001 Exact charge conservation scheme for particle-in-cell simulation with an arbitrary form-factor. *Comput. Phys. Commun.* **135**, 144.

Fukuda, Y., Faenov, A. Ya., Tampo, M., Pikuz, T. A., Nakamura, T., Kando, M., Hayashi, Y., Yogo, A., Sakaki, H., Kameshima, T. *et al.* 2009 Energy increase in multi-mev ion acceleration in the interaction of a short pulse laser with a cluster-gas target. *Phys. Rev. Lett.* **103**, 165002.

Gordeev, A. V. 2010 Nonquasineutral current equilibria as elementary structures of plasma dynamics. *Plasma Phys. Rep.* **36**, 30.

Gu, Y. J., Klimo, O., Kumar, D., Liu, Y., Singh, S. K., Esirkepov, T. Zh., Bulanov, S. V., Weber, S. & Korn, G. 2016 Numerical studies of barotropic modons. *Dyn. Atmos. Oceans* **93**, 013203.

Hasegawa, A. & Mima, K. 1978 Pseudothreedimensional turbulence in magnetized nonuniform plasma. *Phys. Fluids* **21**, 87.

Hide, R. 1983 The magnetic analogue of Ertels potential vorticity theorem. *Ann. Geophys.* **1**, 59.

Hobson, D. D. 1991 A point vortex dipole model of an isolated modon. *Phys. Fluids* B **2** (3), 3027.

Kazimura, Y., Sakai, J. I., Neubert, T. & Bulanov, S. V. 1998 Generation of a small-scale quasi-static magnetic field and fast particles during the collision of electron–positron plasma clouds. *Astrophys. J. Lett.* **498**, 183–186.

KONO, M. & HORTON, W. 1991 Point vortex description of drift wave vortices: dynamics and transport. *Phys. Fluids* B **3**, 3255.

KRASHENINNIKOV, S. I. 2016 On the origin of plasma density blobs. *Phys. Lett.* A **380**, 3905.

KUVSHINOV, B. N. & SCHEP, T. J. 2016 The stability of single and double vortex films in the framework of the Hasegawa–Mima equation. *Plasma Phys. Rep.* **42**, 523.

LARICHEV, V. D. & REZNIK, G. M. 1976 Two-dimensional solitary Rossby waves. *Dokl. Akad. Sci. SSSR* **231**, 12.

LEZHNIN, K. V., KAMENETS, F. F., ESIRKEPOV, T. ZH., BULANOV, S. V., GU, Y. J., WEBER, S. & KORN, G. 2016 Explosion of relativistic electron vortices in laser plasmas. *Phys. Plasmas* **23**, 093116.

LEZHNIN, K. V., KNIAZEV, A. R., SOLOVIEV, S. V., KAMENETS, F. F., WEBER, S. A., KORN, G., ESIRKEPOV, T. ZH. & BULANOV, S. V. 2017 Evolution of relativistic electron vortices in laser plasmas. *Proc. SPIE* **10241**, Y–1.

MCWILLIAMS, J. C., FLIERL, G. R., LARICHEV, V. D. & REZNIK, G. M. 1981 Numerical studies of barotropic modons. *Dyn. Atmos. Oceans* **5**, 219.

NAKAMURA, T., BULANOV, S. V., ESIRKEPOV, T. ZH. & KANDO, M. 2010 High-energy ions from near-critical density plasmas via magnetic vortex acceleration. *Phys. Rev. Lett.* **105**, 135002.

NAKAMURA, T. & MIMA, K. 2008 Magnetic-dipole vortex generation by propagation of ultraintense and ultrashort laser pulses in moderate-density plasmas. *Phys. Rev. Lett.* **100**, 205006.

NASERI, N., BOCHKAREV, S. G., RUAN, P., BYCHENKOV, V. Y., KHUDIK, V. & SHVETS, G. 2018 Growth and propagation of self-generated magnetic dipole vortices in collisionless shocks produced by interpenetrating plasmas. *Phys. Plasmas* **25**, 012118.

NAUMOVA, N. M., KOGA, J., NAKAJIMA, K., TAJIMA, T., ESIRKEPOV, T. ZH., BULANOV, S. V. & PEGORARO, F. 2001 Polarization, hosing and long time evolution of relativistic laser pulses. *Phys. Plasmas* **8**, 4149.

NETTEL, S. 2009 *Wave Physics: Oscillations – Solitons – Chaos*. Springer.

NYCANDER, J. & ISICHENKO, M. B. 1990 Motion of dipole vortices in a weakly inhomogeneous medium and related convective transport. *Phys. Fluids* B **2** (2), 2042.

OVERMAN, E. A. II & ZABUSKY, N. J. 1982 Evolution and merger of isolated vortex structures. *Phys. Fluids* **25** (8), 1297–1305.

PEGORARO, F. 2018 Lorentz invariant 'potential magnetic field' and magnetic flux conservation in an ideal relativistic plasma. *J. Plasma Phys.* **84**, 725840403.

RIDGERS, C. P., KIRK, J. G., DUCLOUS, R., BLACKBURN, T. G., BRADY, C. S., BENNETT, K., ARBER, T. D. & BELL, A. R. 2014 Modelling gamma-ray photon emission and pair production in high-intensity lasermatter interactions. *J. Comput. Phys.* **260**, 273.

ROMAGNANI, L., BIGONGIARI, A., KAR, S., BULANOV, S. V., CECCHETTI, C. A., GALIMBERTI, M., ESIRKEPOV, T. ZH., JUNG, R., LISEYKINA, T. V., MACCHI, A. *et al.* 2010 Experimental observation of organized magnetic vortices in laser–plasma channels. *Phys. Rev. Lett.* **105**, 175002.

SAFFMAN, P. G. 1993 Vortex Dynamics. Cambridge University Press.

SYLLA, F., FLACCO, A., KAHALY, S., VELTCHEVA, M., LIFSCHITZ, A., SANCHEZ-ARRIAGA, G., LEFEBVRE, E. & MALKA, V. 2012 Anticorrelation between ion acceleration and nonlinear coherent structures from laser-underdense plasma interaction. *Phys. Rev. Lett.* **108**, 115003.

WANG, Y. Y., LI, F. Y., CHEN, M., WENG, S. M., LU, Q. M., DONG, Q. L., SHENG, Z. M. & ZHANG, J. 2016 Magnetic field annihilation and reconnection driven by femtosecond lasers in inhomogeneous plasma. *Sci. China Phys. Mech. Astron.* **93**, 013203.

WEI, M. S., BEG, F. N., CLARK, E. L., DANGOR, A. E., EVANS, R. G., GOPAL, A., LEDINGHAM, K. W. D., MCKENNA, P., NORREYS, P. A., TATARAKIS, M. *et al.* 2004 Observations of the filamentation of high-intensity laser-produced electron beams. *Phys. Rev.* E **70**, 056412.

YI, L., PUKHOV, A., SHEN, B., PUSZTAI, I & FÜLÖP, T. 2018 Proton acceleration in a laser-induced relativistic electron vortex. arXiv:1808.04749.

ZHANG, Y. & KRASHENINNIKOV, S. I. 2016 Blobs in the framework of drift wave dynamics. *Phys. Plasmas* **23**, 124501.

https://doi.org/10.1017/S0022377818001162 Published online by Cambridge University Press